

## The structure of heat-resisting alloy modified by thermal treatment and alloyed by rhenium and lanthanum

E V Kozlov<sup>1</sup>, N A Popova<sup>1</sup>, E L Nikonenko<sup>1,2</sup>, A A Kondratyuk<sup>2</sup>, M E Kuznetsov<sup>1</sup> and A A Klopotov<sup>1,3</sup>

<sup>1</sup>Tomsk State University of Architecture and Building, 2, Solyanaya Sq., 634003, Tomsk, Russia

<sup>2</sup>National Research Tomsk Polytechnic University, 30, Lenin Ave., 634050, Tomsk, Russia

<sup>3</sup>National Research Tomsk State University, 36, Lenin Ave., 634050, Tomsk, Russia

E-mail: vilatomsk@mail.ru

**Abstract.** The paper presents the scanning and transmission electron microscope investigations of the structure, phase composition, and morphology of heat-resisting alloy modified by thermal treatment and additionally alloyed by rhenium and lanthanum. Rhenium alloy is obtained by the directional crystallization technique. The structural investigations are carried out for three alloy states, i.e. 1) original (after the directional crystallization); 2) 1150°C annealing during 1 h and 1100°C annealing during 480 h; 3) 1150°C annealing during 1 h and 1100°C annealing during 1430 h. It is shown that fcc-based  $\gamma$ - and  $\gamma'$ -phases are primary in all states of the alloy.  $\gamma'$ -phase has L12 structure, while  $\gamma$ -phase is a disordered phase. Rhenium and lanthanum are phase-forming elements. Investigations show that high-temperature annealing modifies the structural and phase conditions of the heat-resisting alloy.

### 1. Introduction

The properties of heat-resisting nickel alloys are determined for the modern engineering industry by thermal stability of their structure, sizes, shape and amount of strengthening  $\gamma'$ -phase, strength properties of  $\gamma$ -phase solid solution. Usually, such alloys are strengthened by alloying with such phase-forming elements as rhenium and lanthanum. This process increases the operating temperature owing to the melting temperature of forming phases.

### 2. Materials and methods

This paper mainly focuses on the qualitative and quantitative investigations of the structure, phase composition and morphology of heat-resisting alloy additionally alloyed by rhenium Re and lanthanum La both in the original state and after thermal treatment. Three alloy specimens in different states were investigated: 1) original state (after the directional crystallization); 2) original state after 1150°C annealing during 1 h and 1100°C annealing during 480 h; 3) original state after 1150°C annealing during 1 h and 1100°C annealing during 1430 h. All states of the specimens possessed a single-crystal structure with [001] orientation.

The heat-resisting alloy comprised ~70 at.% Ni; ~17 at.% Al and ~5 at.% Cr. The total amount of the primary alloying elements Mo, W, Ta, Ti, Co, Co was ~7 at.% and 0.4 at.% Re and 0.006 at.% La. The concentration of La in specimen 3 was 0.08 at.%.



The scanning electron microscope (SEM) and transmission electron microscope (TEM) investigations were used in this experiment.

### 3. Results and discussion

#### 3.1. Phase composition

TEM investigations show the presence of a number of phases in different states of the alloy the qualitative and quantitative composition of which depends on its thermal treatment (see Table 1).

Phases observed in the alloy are classified into primary and secondary. This classification is based on the volume fraction of phases, their contribution to and stationary or single presence in the alloy. According to Table 1,  $\gamma'$ - and  $\gamma$ -phases are primary. Usually, they form the basic structure of the alloy and are present in the form of  $\gamma'$ -phase quasicuboids layered with  $\gamma$ -phase. All other phases are secondary and formed in individual cases. The volume fractures of phases presented in different states of the alloy are also given in Table 1. The error of determination of the volume fractions is  $\pm 1\%$ . As this Table shows, the volume fracture of  $\gamma'$ -phase keeps high in all states of the alloy. The  $\gamma/\gamma'$  ratio in specimens 1 and 2 is practically similar (0.09 and 0.10, respectively). The introduction of La in specimen 3 in a larger amount reduces  $\gamma/\gamma'$  ratio, because Ni is withdrawn by La more intensively from  $\gamma$ -phase for the formation of  $\text{Ni}_3\text{La}_2$  phase.

In Table 1,  $\beta$ -phase indicates two phases, namely  $\beta$ -NiAl and AlRe [1,2]. These phases possess CsCl structure and can transform to tetragonal phases of  $\text{L1}_0$  type. They are mutually soluble and can form the solid solutions. The presence of  $\beta$ -NiAl and AlRe phases on Ni-Al and Al-Re sides of triangular diagram Ni-Al-Re indicates to their ability to form a large area that connects these positions. Since AlRe-phase has no a specific notation herein, except for its composition,  $\beta$ -NiAl and AlRe phases are denoted by  $\beta$  letter.

**Table 1.** Phase composition and quantitative properties of phases

Phases	Crystal lattice	Space group	Volume fracture, %		
			Specimen 1	Specimen 2	Specimen 3
$\gamma'$	Cuboidal	Pm3m	85.60	90.00	87.00
$\gamma$	Cuboidal	Fm3m	8.00	9.00	6.00
$\gamma/\gamma'$			0.09	0.10	0.07
$\beta$	Cuboidal	$\text{Pm}\bar{3}\text{m}$	5.00	0	0
$\chi$	Cuboidal	$I\bar{4}3\text{m}$	1.40	0	0
$\sigma$	Tetragonal	$\text{P4}_2/\text{mmn}$	0	1.00	2.00
$\text{La}_2\text{Ni}_3$	Orthorombic	$\text{Cmca}$	0	0	5.00

According to Table 1,  $\sigma$  and  $\chi$  phases relate to Frank-Kasper phases or topologically close-packed phases [1,2]. These phases are formed due to Re presence in the alloy. Actually, the interaction of Re with Mo and W results in the formation of  $\sigma$  and  $\chi$  phases. The former one results from high-temperature hardening of the solid solution, the latter one results from its low-temperature breakdown and crystallization. Moreover,  $\sigma$ -phase is formed as a result of Re interaction with Co, Cr, Ni, Al, while  $\chi$ -phase results from Re interaction with Mo and W as well as with Co and Al.

Finally,  $\text{Ni}_3\text{La}_2$  phase is formed just in La-alloyed alloy in a larger amount, i.e. in specimen 3 (see Table 1). Except for this phase, other phases are represented by concentrated solid solutions observed in a wide concentration range and involved in all phase transformations.

#### 3.2. Phase morphology

As it is known, the structure of superalloys is represented, first of all, by  $(\gamma+\gamma')$ -phase mixture. A presence of such active metals as Re and La in superalloy, complicates its structure and leads to the

formation of areas with damaged  $(\gamma+\gamma')$ -structure [3-5]. Due to Re,  $\beta$ -phase is formed partially, while  $\sigma$  and  $\chi$  phases are formed completely. The introduction of La promotes the formation of  $\text{Ni}_3\text{La}_2$  phase (see Table 1). The formation of these four phases results in a serious damage of the quasi-cuboidal structure of  $(\gamma+\gamma')$ -phases. Since the distribution of Re and La in the alloy is not uniform, only a part of  $(\gamma+\gamma')$ -phase quasi-cuboids is damaged. The experimental research has assisted in schematic representation of the specimens' structure given in Figures 1-3.

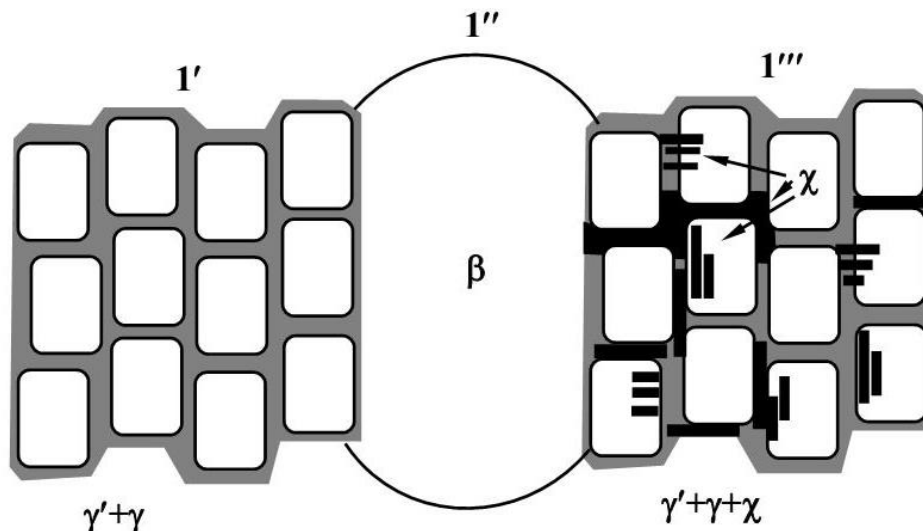


**Figure 1.** Schematic representation of specimen #1 structure: three states of phase morphology:  $1'$  – ideal structure of  $(\gamma+\gamma')$ -phase quasi-cuboids;  $1''$  – a part of  $\beta$ -phase;  $1'''$  –  $(\gamma+\gamma')$ -phase quasi-cuboids with  $\chi$ -phase layers

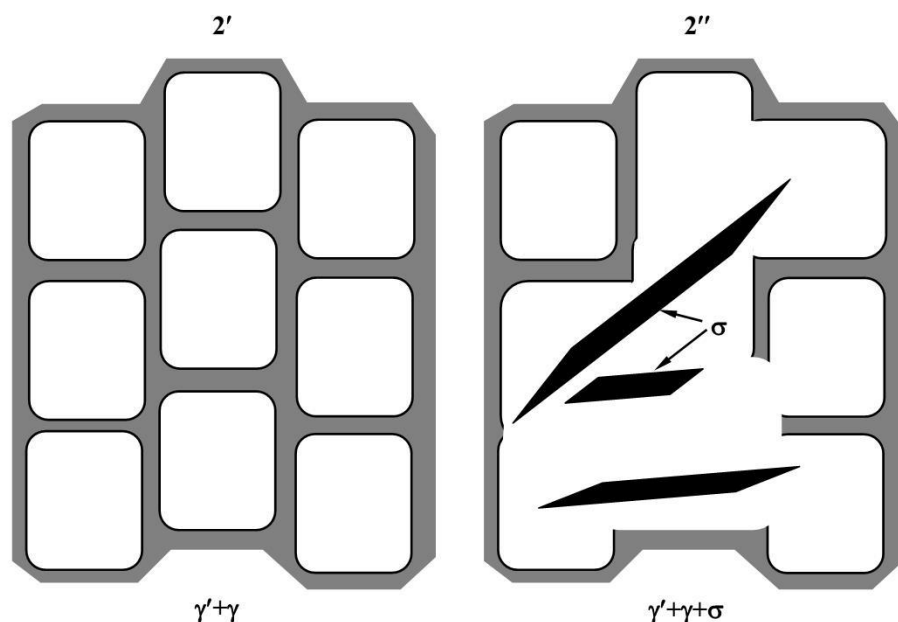


**Figure 2.** Schematic representation of specimen #2 structure: two states of phase morphology:  $2'$  – ideal structure of  $(\gamma+\gamma')$ -phase quasi-cuboids;  $2''$  –  $(\gamma+\gamma')$ -phase quasi-cuboids with  $\sigma$ -phase separations

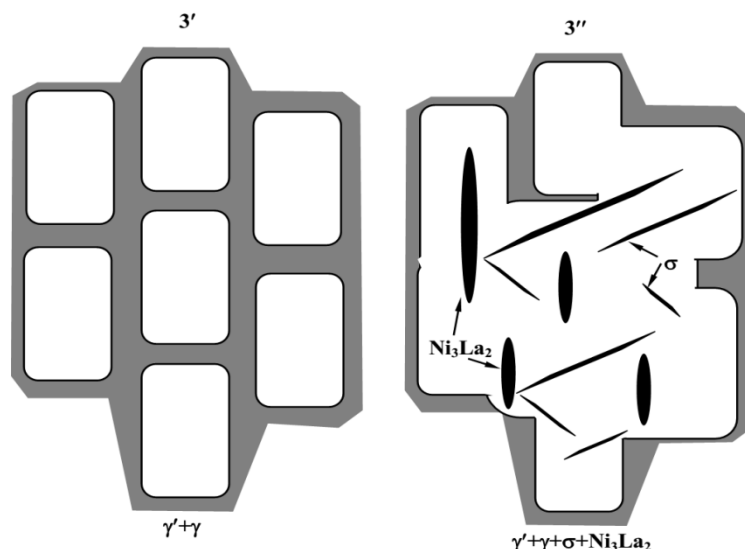


**Figure 3.** Schematic representation of specimen #3 structure: two states of phase morphology: 3' – ideal structure of  $(\gamma+\gamma')$ -phase quasi-cuboids; 3'' –  $(\gamma+\gamma')$ -phase quasi-cuboids with  $\sigma$ -phase and  $\text{Ni}_3\text{La}_2$  separations.

**3.2.1. Specimen 1.** Three states 1', 1'' and 1''' of phase morphology are schematically represented in Figure 1. State 1' is the ideal structure of  $(\gamma+\gamma')$ -phase quasi-cuboids with a slightly anisotropic distortion. Along with  $(\gamma+\gamma')$ -phase quasi-cuboids, state 1''' includes  $\chi$ -phase layers. These layers are localized both in  $\gamma'$ - and  $\gamma$ -phase. The orientation of these layers is parallel to the cuboid orientation of  $\gamma'$ - and  $\gamma$ -phases as well as that of  $\gamma$ -phase layers. Quasi-cuboids in state 1''' are also anisotropic. Figure 4 contains TEM images of states 1', 1'' and 1'''.

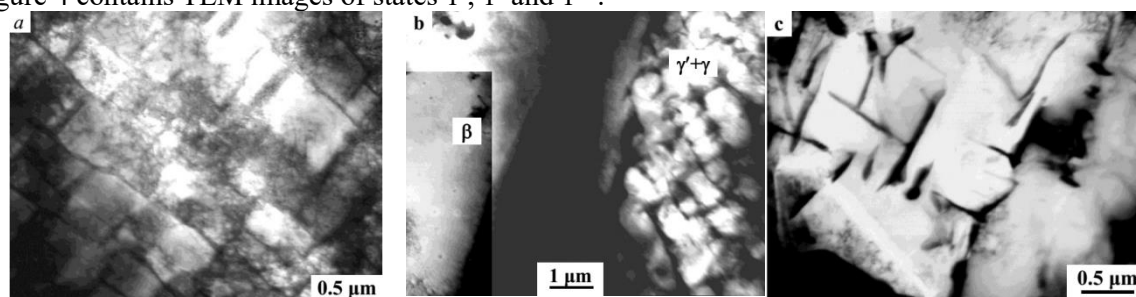
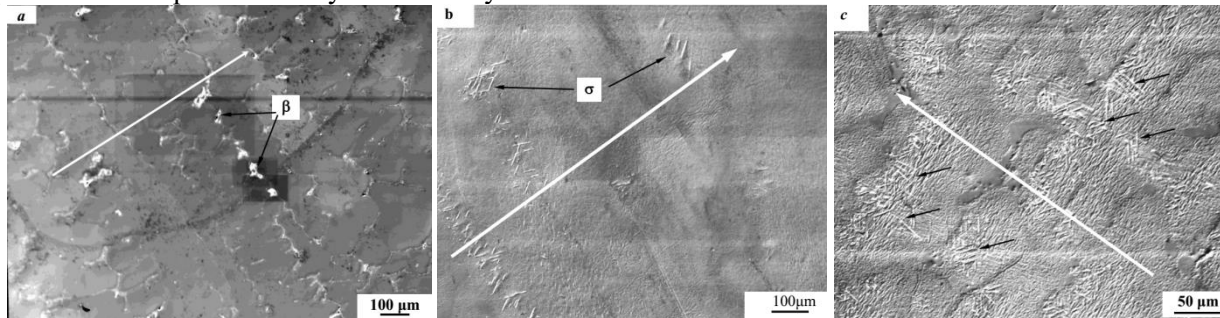


**Figure 4.** TEM image of specimen #1 structure: *a* - quasi-cuboidal structure of  $(\gamma+\gamma')$ -phases (state 1'); *b* - intersection of 1' ( $\gamma'+\gamma$ ) and 1'' ( $\beta$ ) states; *c* - state 1''' ( $\chi$ -phase layers are observed)

State 1'' presented in Figure 4 b, is characterized by a completely damaged structure of quasi-cuboids, or rather they are absent. The area of state 1'' is fully occupied, at least, by the three-component solution of  $\text{NiAl}_2\text{Re}$ . The latter is a chemical formula of the three-component  $\beta$ -phase. The intersection of this phase and  $(\gamma+\gamma')$ -phase mixture shown in Figure 4 b, has  $[011]$  direction of  $\gamma'$ -phase. The orientation relation between  $\beta$ -phase and  $\gamma/\gamma'$ -phases is  $[110]\beta \parallel [111]\gamma'$ . This relation is typical for the mutual phase transformation of  $\text{fcc} \rightarrow \text{bcc}$ . In Figure 4 c, the layers of  $\gamma'$ - and  $\chi$ -phases are parallel. The both phases possess a cubical lattice; their size effects provide a certain crystallographic misorientation.

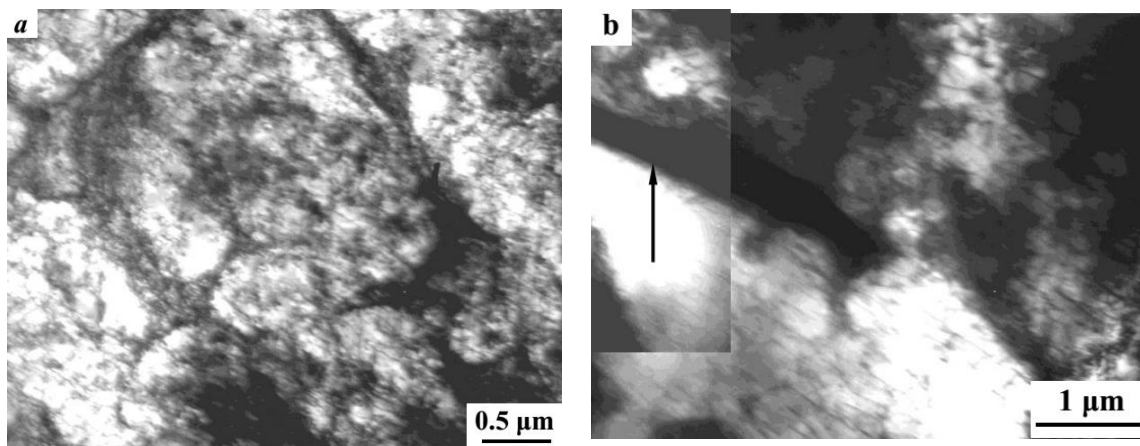
The SEM images of specimens #1-3 structure are presented in Figure 5. In Figure 5a, the larger volume of the alloy is occupied by quasi-cuboids, both damaged and not damaged. Because of low

image magnification, their contrasts do not differ. Rhenium layering is clear due to the separation of  $\beta$ -phase which is predominately stabilized by this element.



**Figure 5.** SEM images of alloy structure: *a* – specimen 1. Black arrows emphasize  $\beta$ -phase particles; *b* – specimen 2. Black arrows emphasize  $\sigma$ -phase particles; *c* - specimen 3. Black arrows emphasize La and  $\sigma$ -phase particles. White arrows emphasize the regular structure.

3.2.2. *Specimen 2.* From the schematic representation of the structure of specimen #2 shown in Figure 2, the alloy comprises  $(\gamma+\gamma')$ -phase quasi-cuboids of the ideal structure with the volume fracture of 0.9 and  $(\gamma+\gamma')$ -phase quasi-cuboids distorted by  $\sigma$ -phase with 0.1 volume fracture. Let denote these structural and phase conditions as state 2' and state 2''. TEM images of these states are shown in Figure 6.



**Figure 6.** TEM images of  $(\gamma+\gamma')$ -phase quasi-cuboids in specimen 2: *a* – state 2'; *b* – state 2''. Black arrows emphasize  $\sigma$ -phase particles

The elongated particles of  $\sigma$ -phase are localized in  $[011]$  and  $[001]$  directions of  $\gamma'$ -phase. The  $\gamma'$ - and  $\sigma$ -phase intersection is not rather distorted. This fact can be proved by the absence of bend extinction contours in the alloy structure. As shown in Figure 6b, in  $\sigma$ -phase the quasi-cuboid structure is distorted. The effect from the local formation of secondary phases in specimen #2 is more explicit than in specimen 1. Thus, the volume fracture of ideal quasi-cuboids is 0.65 for specimen #1 and 0.9 for specimen #2.

The SEM image of the structure of specimen #2 is presented in Figure 5b. The local distribution of  $\sigma$ -phase particles alternates with the ideal structure of  $(\gamma+\gamma')$ -phases. Thus, a good correlation is observed between SEM and TEM investigations.

3.2.3. *Specimen #3.* According to the schematic representation of specimen #3 given in Figure 3, the ideal quasicuboids occupy just over half (0.55) of the material (state 3') and 0.45 volume fracture belongs to  $(\gamma' + \gamma + \sigma + \text{Ni}_3\text{La}_2)$ -phase mixture (state 3''). TEM images of these states are presented in Figure 7. The volume fractures of these both states are comparable. The volume fracture of  $\text{Ni}_3\text{La}_2$ -

phase is larger than that of  $\sigma$ -phase. This is because the additional specimen alloying with La. Moreover, the amount of  $\sigma$ -phase in specimen #3 is larger than in specimen #2. This can be connected both with a longer period of thermal treatment and the indirect influence of La on phase formation. Another interesting fact is that the separation of  $\sigma$ -phase and  $\text{Ni}_3\text{La}_2$ -phase occurs in the same locality. Figure 7b shows that particles of  $\sigma$ -phase have always an acicular shape, while particles of  $\text{Ni}_3\text{La}_2$ -phase always have the internal structure with a characteristic contrast and finite thickness.

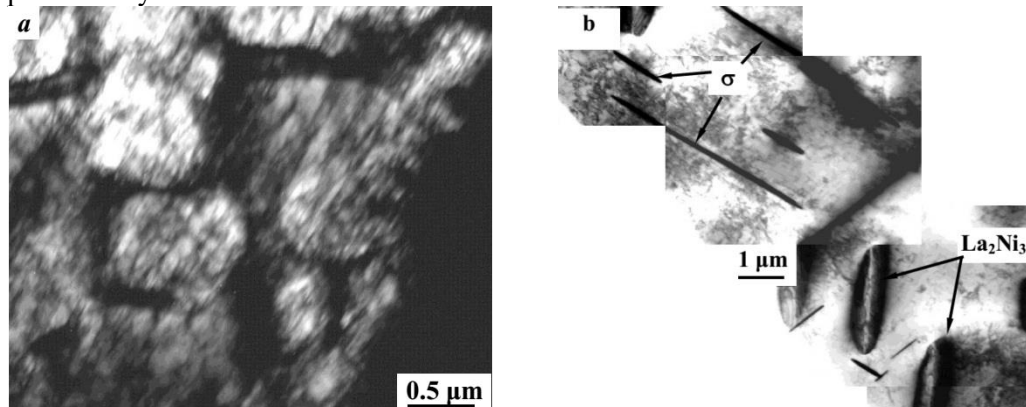


**Figure 7.** TEM images of specimen #3: *a* – state 3'; *b* – state 3''. Black arrows emphasize secondary phases

The SEM investigations of etched surfaces of specimen #3 shown in Figure 5 c, prove the data obtained as a result of TEM investigations, namely: the presence of two states of the structural and phase conditions (states 3' and 3'') that have a regular structure; the comparability of volume fractures of states 3' and 3''.

#### 4. Conclusion

The investigations showed that the introduction of La in the alloy phase composition restrains the formation of  $\gamma$ -phase. Particles of  $\text{Ni}_3\text{La}_2$ -phase have a platelike shape and are localized in certain areas of the alloy. Rhenium and lanthanum alloying resulted in the formation of heat-resisting phases such as  $\beta$ -,  $\sigma$ -, and  $\chi$ -phases ( $\sim 1600$ ,  $\sim 2600$ ,  $\sim 2800^\circ\text{C}$  melting temperature respectively) that promote the strengthening of the alloy.

#### Acknowledgement

The authors acknowledge the partial financial support from the Russian Foundation for Basic Research Project 16-48-700198 and the partial financial support from project (No. 8.1.42.2015) within the framework of the Program “Scientific Foundation named after D.I. Mendeleev of Tomsk State University” in 2015-2016.

#### References

- [1] Kolobov Yu R, Kablov E N and Kozlov EV 2008 *Structure and properties of intermetallic materials with nano-phase hardening* (Moscow, MISiS) (in Russian)
- [2] Kozlov E V, Smirnov A N, Nikonenko E L, Popova N A and Koneva N A 2016 *Phase morphology and transformations due to thermal treatment of Ni-Al-Cr Ni-Al-Co-based superalloys. Scale and concentration effects* (Moscow, Innovatsionnoe mashinostroenie) p 175 (in Russian)
- [3] Sugui T, Minggang W, Huichen Y, Xingfu Y, Tang L and Benjiang 2010 *Materials Science and Engineering A* **527** 4458
- [4] Pyczak F, Neumeier S and Goken M 2010 *Materials Science and Engineering A* **527** 7939
- [5] Neumeier S, Pyczak F and Goken M 2011 *Philosophical Magazine* **91** 33 4187